

Cover Page



Universiteit Leiden



The handle <http://hdl.handle.net/1887/28971> holds various files of this Leiden University dissertation

Author: Rosalia, Rodney Alexander

Title: Particulate based vaccines for cancer immunotherapy

Issue Date: 2014-10-02

Chapter 7

CD40-targeted dendritic cell delivery of PLGA-nanoparticle vaccine induce potent anti-tumor responses

Rodney A. Rosalia*, Luis Javier Cruz*, Suzanne van Duikeren, Angelino Tromp, Ana Luisa Silva, Wim Jiskoot, Tanja de Gruijl, Clemens Löwik, Jaap Oostendorp, Sjoerd H. van der Burg, Ferry Ossendorp

* Contributed equally to this study

Submitted for publication

Abstract

Dendritic cells (DC) play a prominent role in the priming of CD8⁺T cells. Vaccination is a promising treatment to boost tumor-specific CD8⁺T cells which is crucially dependent on adequate delivery of the vaccine to DC. Upon subcutaneous (s.c.) injection, only a small fraction of the vaccine is delivered to DC whereas the majority is cleared by the body or engulfed by other immune cells.

To overcome this, we studied vaccine delivery to DC via CD40-targeting using a multi-compound particulate vaccine with the aim to induce potent CD8⁺T cell responses. To this end, biodegradable poly(lactic-co-glycolic acid) nanoparticles (NP) were formulated encapsulating a protein Ag, Pam3CSK4 and Poly(I:C) and coated with an agonistic α CD40-mAb (*NP-CD40*). Targeting NP to CD40 led to very efficient and selective delivery to DC *in vivo* upon s.c. injection and improved priming of CD8⁺T cells against two independent tumor associated Ag. Therapeutic application of *NP-CD40* enhanced tumor control and prolonged survival of tumor-bearing mice.

We conclude that CD40-mediated delivery to DC of NP-vaccines, co-encapsulating Ag and adjuvants, efficiently drives specific T cell responses, and therefore, is an attractive method to improve the efficacy of protein based cancer vaccines undergoing clinical testing in the clinic.

Introduction

Dendritic Cells (DC) are the main antigen (Ag) presenting cells (APC) of the immune system^{1,2} and their ability to orchestrate innate and adaptive immunity is widely being exploited to develop cancer immunotherapies³. Immature DC have high endocytic capacity, express various intra- and extracellular pathogen recognition receptors, such as toll-like receptors (TLR), and continuously sample their surroundings for danger signals. TLR-triggering results in phenotypical changes, facilitated Ag processing, MHC presentation and increased cytokine production, a process termed DC maturation⁴.

Therapeutic vaccinations against cancer are centered on the delivery of tumor associated Ag (TAA) to DC which then initiate Ag-specific T cell responses^{5,6}. However, *in vivo* generation of robust anti-tumor cytotoxic CD8⁺ T cells (CTL) remains a major challenge. Targeted delivery of TAA to DC using nanoparticle (NP) vaccine carriers formulated with poly(lactic-co-glycolic acid) (PLGA) is an attractive approach to enhance specific T cell responses. PLGA NP can be formulated to encapsulate protein⁷ or short-⁸ and long-peptide⁹ Ag encoding TAA and TLR ligands (TLRL)¹⁰. Encapsulation of Ag in NP facilitates MHC Ag presentation⁸ and *in vivo* anti-tumor T cell responses compared to soluble Ag¹¹. Encapsulation of Ag in NP facilitates MHC Ag presentation and *in vivo* anti-tumor T cell responses compared to soluble Ag.

Due to their physical characteristics, NP are prone to be internalized by scavenger cells, such as macrophages (M ϕ), which offer poor T cell priming capacity compared to DC. Protection from nonspecific uptake is achieved by pegylation of NP which also prolongs the *in vivo* half-life¹². Pegylated NP can be specifically (re-)targeted to DC by additional surface modifications which is suggested to enhance *in vivo* T cell responses. Indeed, C-type lectin specific antibodies coated to PLGA-PEG NP^{13,14} but also compounds such as protamine and mannose coated to the PLGA-NP surface core^{15,16} have been shown to improve *in vitro* binding and internalization by DC and promote better T cell responses. However, no direct evidence was provided in these studies for selective DC-targeting and improved delivery of the vaccine to DC *in vivo*.

Facilitating *in vivo* delivery of PLGA-NP-vaccines to DC via CD40 and the resulting vaccine induced T cell responses is the subject of this study. CD40 is a tumor necrosis factor-receptor family cell surface receptor highly expressed on DC. CD40/CD40L ligation plays a crucial role in the maturation of DC into fully competent APC and is a key signal for CD4⁺ T helper dependent CD8⁺ T cell priming^{17,18}. Moreover, targeting soluble Ag via CD40 using antibody

constructs was shown to facilitate the internalization of Ag into early-endosomes¹⁹, intracellular compartments associated with efficient MHC class I Ag cross-presentation, and promotes tumor-specific T cell responses²⁰.

In this study, we evaluated CD40-targeting of a particulate Ag, by formulating PLGA-NP co-encapsulating ovalbumin protein, the adjuvants Pam3Csk4 (TLR2L) and Poly(I:C) (TLR3L), as well as the murine α CD40-mAb FGK45¹⁷ coupled to the NP-surface, PLGA(-Ag/TLR2+3L)- α CD40 (*NP-CD40*).

We report here, that *NP-CD40* administered as a vaccine displays selective and improved capacity to deliver Ag to DC *in vivo*, over other APC, and better DC maturation in comparison to non-targeted NP-vaccines. Vaccinations with *NP-CD40* resulted in the priming of robust Ag-specific CD8⁺ T cells with the capacity to control tumor growth and prolong survival of tumor-bearing animals.

Material and methods

Animals

C57BL/6 (CD45.2/Thy1.2; H-2^b) mice were obtained from Charles River Laboratories. Ly5.1/CD45.1 (C57BL/6 background), CD40 KO (C57BL/6 background), transgenic OT-I/Thy1.1/CD45.2 (specific for the OVA₂₅₇₋₂₆₄ CTL epitope presented by H2-K^b) and transgenic OT-II/Ly5.1/CD45.1 mice (specific for the OVA₃₂₃₋₃₃₉ Th epitope presented by I-A^b) were bred in the specific pathogen-free animal facility of the Leiden University Medical Center. All animal experiments were approved by the animal experimental committee of Leiden University.

DC and cell lines

Mouse BMDC were cultured published previously¹⁸. In brief, Freshly isolated mouse bone marrow (BM) cells from WT C57BL/6 mice or CD40 KO femurs were and cultured for 10 days in medium supplemented with GM-CSF (50 ng/ml). After 10 days of culture, large numbers of typical DC were obtained which were at least 90% positive for murine DC marker CD11c (data not shown). D1 cells, a GM-CSF dependent immature dendritic cell line were cultured as described before²¹. OVA-transfected B16 tumor cell line (B16-OVA), syngeneic to the C57BL/6 strain, was cultured as described previously²².

Preparation and characterization of targeted PLGA-NP

PLGA-NP (Ag/TLRL)-mAb were formulated encapsulating a model protein Ag and in combination with TLR2L (Pam3Csk4) and/or TLR3L (Poly(I:C)) using double-emulsion and solvent evaporation technique as previously described²⁰. PLGA-NP was coated with mAbs, murine agonistic α CD40 mAb, FGK45 and mouse IgG2a Isotype control respectively, essentially as described before²³. In brief, 100 mg of PLGA in 2 mL of ethyl acetate containing OVA antigen free from endotoxin (10 mg) and/or Poly(I:C) (InvivoGen) (4 mg) and/or Pam3CSK4 (InvivoGen) (1 mg) were emulsified under sonification (Branson, sonifier 250) during 60 seconds. This first emulsion was rapidly added to 1 mL of 1% polyvinyl alcohol/7% ethyl acetate in distilled water during 15 second. A combination of pegylated lipids (DSPE-PEG(2000) succinic acid (6 mg) and mPEG 2000 PE (6 mg)) were dissolved in chloroform and added to the vial. The chloroform was removed by a stream of nitrogen gas. Subsequently, the emulsion was rapidly added to the vial containing the lipids and the solution was homogenized during 30 seconds using a sonicator. This solution was added to 100 mL of 0.3% PVA/7% of ethyl acetate in distilled water and stirred overnight to evaporate ethyl acetate. The PLGA-NP were collected by centrifugation at 12000 x g for 10 min, washed four times with distilled water and lyophilized. Next, mAbs was covalently coupled to 10 mg of PLGA-NP by activating surface carboxyl groups in isotonic 0.1 M MES buffer pH 5.5 containing 1-ethyl-3-[3-dimethylaminopropyl] carbodiimide hydrochloride (10 equiv.) and N-hydroxysuccinimide (10 equiv.) for 1 h. Mouse IgG2a Isotype control (Clone:C1.18.4 Catalog #:BE0085) was purchased from Bio X Cell Antibody Production and Purification. The activated carboxyl-PLGA-NP was washed one time with MES buffer by centrifugation. Subsequently, mAbs (200 μ g per mg NP) were added and the suspension was stirred during 3 h at room temperature and later overnight at 4°C. Unbound antibodies were removed by centrifugation (12000 x g, during 10 min) and the PLGA-NPs-mAbs was washed four times with PBS. The presence of Abs on the particle surface was determined by Coomassie dye protein assay. Physicochemical characteristics of formulated NP are summarized in Table 7.1.

Dynamic light scattering and zeta-potential measurements

Dynamic light scattering (DLS) measurements were taken on different PLGA-NP using an ALV light-scattering instrument equipped with an ALV5000/60X0 Multiple Tau Correlator and an Oxixus SLIM-532 150 mW DPSS laser operating at a wavelength of 532 nm. A

Table 7.1 Physicochemical characteristics of formulated PLGA-NP

Samples	Poly(I:C) Pam3Csk4 ($\mu\text{g}/\text{mg NP}$) (w/w)	Ag ($\mu\text{g}/\text{mg NP}$) (w/w)	Nanoparticles dm \pm S.D. (nm)	Polydispersity index \pm S.D.	Zeta potential \pm S.D. (mV)	Coated mAb ($\mu\text{g}/\text{mg PLGA-NP}$)
PLGA-(OVA)-IgG2a	---	40.0	240.6 \pm 13.5	0.136 \pm 0.053	-35.4 \pm 6.2	23.0 \pm 2.9
PLGA-(OVA)- α CD40	---	40.0	233.7 \pm 8.3	0.139 \pm 0.045	-31.2 \pm 5.2	29.1 \pm 3.1
PLGA-(OVA/TLR3L)-Ig2a	15.0	55.1	198.2 \pm 12.9	0.085 \pm 0.016	-33.6 \pm 5.5	32.0 \pm 3.2
PLGA-(OVA/TLR3L)- α CD40	15.0	55.1	194.7 \pm 11.6	0.148 \pm 0.068	-30.0 \pm 4.6	25.0 \pm 3.7
PLGA-(OVA/TLR2L)-Ig2a	4	64	192.1 \pm 11.3	0.097 \pm 0.046	-32.2 \pm 2.5	34.0 \pm 2.4
PLGA-(OVA/TLR2L)- α CD40	4	64	195.4 \pm 14.3	0.122 \pm 0.049	-31.0 \pm 4.6	29.0 \pm 3.2
PLGA-(OVA/TLR2+3L)-Ig2a	45 4	60	241.4 \pm 16.7	0.159 \pm 0.033	-36.3 \pm 1.6	35.0 \pm 3.1
PLGA-(OVA/TLR2+3L)- α CD40	45 4	60	242.3 \pm 25.0	0.167 \pm 0.031	-38.5 \pm 1.7	32.0 \pm 2.2
PLGA-(OVA-Alexa647/TLR2+3L)-Ig2a	16 4	12	212.2 \pm 10.4	0.121 \pm 0.027	-31.4 \pm 2.3	34.5 \pm 3.2
PLGA-(OVA-Alexa647/TLR2+3L)- α CD40	16 4	12	209.8 \pm 11.1	0.114 \pm 0.022	-32.2 \pm 2.8	31.3 \pm 1.8
PLGA-(HPV-E7/TLR2+3L)-Ig2a	15 4	12	239 \pm 13.6	0.234 \pm 0.072	-29.6 \pm 1.8	34.4 \pm 1.4
PLGA-(HPV-E7/TLR2+3L)- α CD40	15 4	12	246 \pm 16.1	0.204 \pm 0.062	-28.5 \pm 2.1	29.0 \pm 1.9

refractive index matching bath of filtered cis-decalin surrounded the cylindrical scattering cell, and the temperature was controlled at 21.5 ± 0.3 °C using a Haake F3-K thermostat. In each sample, the $g_2(\tau)$ auto-correlation function was recorded ten times at a detection angle of 90°. For each measurement, the diffusion coefficient (D) was determined by using the second-order cumulant, and the corresponding PLGA-NP diameter was calculated assuming that the PLGA-NP were spherical in shape. Zeta potential measurements were performed on PLGA-NP using a Malvern ZetaSizer 2000 (UK).

Quantifying encapsulated OVA in NPs

OVA-protein encapsulating efficiency was determined after hydrolyzing 5 mg PLGA-NPs in 0.5 mL 0.8 M NaOH overnight at 37°C. The OVA-protein content was then measured using Coomassie Plus Protein Assay Reagent (Pierce) according to the manufacturer's protocol. OVA encapsulation efficiency was calculated by dividing the measured amount of encapsulated Ag by the theoretical amount assuming all was encapsulated.

Quantifying encapsulated TLR ligands

Biodegradable PLGA-NP was hydrolyzed with 0.8 M NaOH overnight at 37°C. The encapsulation efficiency of Poly(I:C) was determined by reversed-phase high-performance liquid chromatography (RP_HPLC) and was also determined by UV spectrometry using a Nanodrop system (Thermo Scientific). Poly(I:C) was assayed by RP-HPLC at room temperature using a Shimadzu system (Shimadzu Corporation, Kyoto, Japan) equipped with a reversed-phase Symmetric C18 column (250 mm x 4.6 mm). The flow rate was fixed at 1 mL/min and detection was obtained by UV detection at 254 nm. A linear gradient of 0% to 80% of acetonitrile (containing 0.036% trifluoroacetic acid) in water (containing 0.045% trifluoroacetic acid) was used for Poly(I:C). The retention time of the Poly(I:C) was approximately 20 min. The regression analysis was constructed by plotting the peak-area ratio of Poly(I:C) versus concentration. The calibration curves were linear within the range of 2.5 µg to 150 µg for Poly(I:C). The correlation coefficient (R^2) was greater than 0.99.

Analysis of *in vitro* NP-association with DC

WT C57BL/6 or CD40 KO BMDC (100,000/well) were plated into a 96-well flat bottom plate and incubated for 1 hr at either 4°C (binding analysis) or 37°C (uptake analysis) with titrated

amounts of CD40-targeted or non-targeted (PLGA-Ag/TLR2+3L)-PEG-mAb formulations labeled with the near infrared dye (near-IR dyes, CW800). Cells were washed twice to remove residual non-bound NP. Binding and uptake of PLGA-NP by DC was determined based on near-IR fluorescence using odyssey equipment (LI-COR) at 800 nm. Data analyses were corrected for the number of amount cells per measurement via co-staining with TO-PRO® (Invitrogen) at 700 nm.

Analysis of *in vivo* NP-uptake by immune cells

Animals were vaccinated with the CD40-targeted or non-targeted (PLGA-Ag/TLR2+3L)-PEG-mAb formulations containing OVA-Alexa647 (Invitrogen) by subcutaneous (s.c.) injection into the right flank. *In vivo* NP-uptake by cells was analyzed 24 or 48 hr after vaccination by sacrificing the animals and isolating the inguinal lymph nodes. Single cell suspensions were prepared and flow cytometry was used to determine the fluorescence intensity of OVA-Alexa647 in F4/80-CD11b⁺CD11c⁺ DC and CD19⁺B220⁺ B cells as a measure for NP-uptake. All fluorescent-mAb used for staining were purchased from BD Pharmingen. Flow cytometry was performed using a LSRII (BD Pharmingen) and data analyzed with FlowJo software (Treestar).

***In vitro* MHC class II-restricted Ag presentation and T cell priming**

DC were incubated for 5 hr with the various (PLGA-Ag/TLRL)-mAb formulations at the indicated OVA concentrations. After incubation, supernatants were harvested and cells were then further co-cultured for 72 hr in the presence of OT-II splenocytes to assess OVA-specific MHC class II-restricted proliferation of naïve CD4⁺ T cells. Cells were pulsed with [³H]-thymidine for the last 16 hours of culture. Samples were then counted on a TopCount™ microplate scintillation counter (Packard Instrument Co., Meridan, CT, USA). Stimulation index was used as a measure for proliferation and was calculated as the fold increase of [³H]-thymidine CPM over the CPM counts obtained with medium as negative control.

Analysis of cytokine production by DC or T cells using Enzyme-linked Immunosorbent Assay (ELISA)

DC (100,000/well) were plated into a 96-well round bottom plate and incubated for 24 hr with titrated amounts of Ag. Supernatants were harvested and tested for IL-12 p70 by ELISA (BD OptEIA™ MOUSE IL-12 Cat. Nr 555256) following the manufacturer's instructions.

Vaccination and immunization schemes

Animals were vaccinated with the various targeted or non-targeted NP formulations (Table 7.1) by s.c. injection into the right flank. *In vivo* priming of cytotoxic CD8⁺ T cells was studied 1 week post-vaccination by transferring splenocytes prepared from congenic Ly5.1 C57BL/6 animals which were pulsed with the SIINFEKL (OVA₈/specific target cells) or ASNENMETM (FLU9/non-specific target cells) short peptide. The target cells were labeled with either 10 μM (OVA) or 0.5 μM (Flu) CFSE mixed 1:1 and 10⁷ total cells were injected intravenously (i.v.) into vaccinated animals. 18 hr post transfer of target cells, animals were sacrificed and single cell suspensions were prepared from isolated spleens. Injected target cells were distinguished by APC-conjugated rat anti-mouse CD45.1 mAb (BD Pharmingen). *In vivo* cytotoxicity was determined by flow cytometry using the following formula: $(1 - [(CFSE\text{-peak OVA}/CFSE\text{-peak FLU})^{\text{vaccinated animals}} \times (CFSE\text{-peak OVA}/CFSE\text{-peak FLU})^{\text{non-vaccinated animals}}]) \times 100\%$. Vaccine efficacy against the HPV-E7 oncoprotein was determined in blood of TC-1 tumor bearing mice (60000/TC-1 cells per mice inoculated s.c. in the left flank). Mice were vaccinated on day 7 with 15 μg HPV-E7 protein encapsulated in CD40-targeted NP, control formulations or in soluble form and HPV-E7 -specific CD8⁺ T cell responses were measured by quantification via flow cytometry of RAHYNIVTF/H2-D^b-TM (APC-labeled) positive CD8⁺ T cells co-stained with AF-conjugated anti-mouse CD8α mAb and V500-conjugated rat anti-mouse CD3 mAb.

Tumor challenge

Therapeutic and prophylactic vaccine capacity of CD40-targeted NP and relevant controls were studied by analyzing their efficiency to induce anti-tumor immune responses. For prophylactic tumor challenges mice were vaccinated s.c. in the right flank and seven days later OVA-expressing melanoma cells (B16-OVA) were inoculated s.c. on the opposite flank. Tumor size (mm³) was calculated by $(\text{length}) \times (\text{width}) \times (\text{length} + \text{width}/2)$. Animal survival was then followed and mice were sacrificed when humane end-points were met as described in Code of practice for animal experiments in oncological related research (*Code of practice dierproeven in het kankeronderzoek*).

To assess the therapeutic capacity of CD40-targeted NP we inoculated 2 × 10⁵ B16-OVA melanoma cells s.c. in the right flank of WT C57BL/6 mice. On day 7 and day 17 post tumor inoculation, mice were s.c. vaccinated with 10 μg of OVA encapsulated in PLGA-(OVA/TLR2+3L)-αCD40 and PLGA-(OVA/TLR2+3L)-IgG2a NP (12 mice per group) on the opposite

flank. Tumor growth was measured 1–3 times a week and survival was monitored daily. Tail vein blood samples were collected on day 14 after tumor challenge. Blood samples were prepared by erythrocyte lysis, followed by 2 washing steps with PBA buffer. OVA-specific CD8⁺ T cells were analyzed by co-staining with APC-conjugated SIINFEKL/H2-K^b tetramers (TM), AF-conjugated anti-mouse CD8 α mAb and V500-conjugated rat anti-mouse CD3 mAb. All fluorescent-antibodies used for staining were purchased from BD Pharmingen and the APC-SIINFEKL/H2-Kb tetramers were produced in house. Flow cytometry analysis was performed as described above.

Statistical analysis

Graph Pad Prism software version 5 was used for statistical analysis. Two-way analysis of variance (ANOVA) tests were used to evaluate cytokine production by DC or T cells across different concentrations of PLGA-(OVA/TLR)-mAb and to analyze differences in *in vitro* binding/uptake studies. The differences in OVA-Alexa647 fluorescence upon *in vivo* uptake by immune cells were analyzed using the two-tailed unpaired Students t test or Mann Whitney test. Dose-response *in vitro* studies were analyzed using two-way ANOVA with Bonferroni posttests. Differences in animal survival were calculated using Log-rank (Mantel-Cox) test. Statistical significance was considered when $P < 0.05$.

RESULTS

Coupling of α CD40-mAb to NP improves binding and internalization by DC *in vitro* and *in vivo*

The efficiency of targeting via CD40 was analyzed by determining the efficacy of binding and internalization of NP by DC. Two types of formulations were compared and unless otherwise stated PLGA-(Ag/TLR2+3L)- α CD40 NP are referred to as *NP-CD40* and PLGA-(Ag/TLR2+3L)-IgG2a (NP) as *NP-Iso* (IgG2a-isotype control mAb coated NP). DC were incubated for 1 hr with fluorescently labeled NP at 4°C (binding) and 37°C (internalization). Coupling of the α CD40-mAb significantly improved the association of NP with DC compared to isotype control mAb (Figure 7.1). The effect of CD40-targeting was also observed in a mixed cell culture. *NP-CD40* added to spleen single cell suspensions *in vitro* were internalized better by DC than B cells (Supporting Information Figure S7.1). But F4/80⁺CD11b⁺CD11c⁻ M ϕ showed poor capacity to take up NP, irrespective of targeting (data not shown).

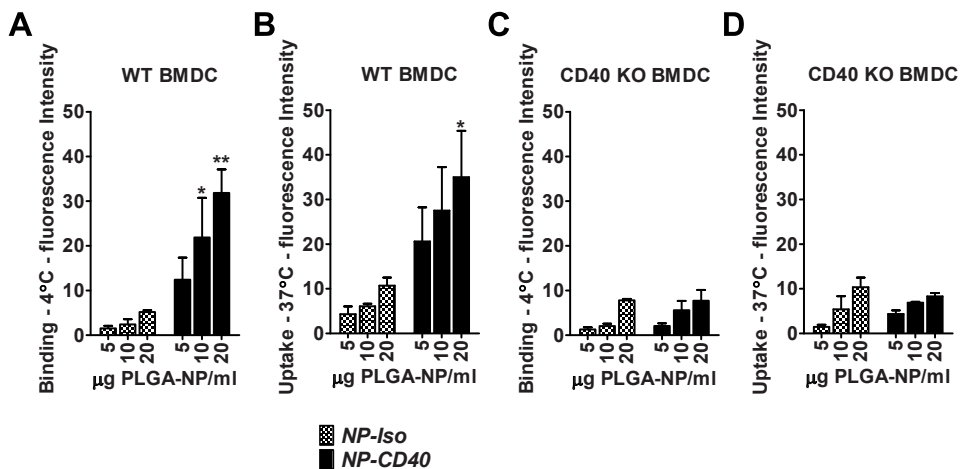


Figure 7.1 DC more efficiently binds and internalizes NP-CD40 compared to NP-Iso.

WT BMDC were incubated with titrated amounts of NP-CD40 or NP-Iso for 1 hr at 4°C to study binding (A) or 37°C for uptake (B) followed by extensive washing with medium to remove unbound NP. CD40-mediated binding and uptake of NP was tested CD40 KO BMDC (C & D). Fluorescence intensity was measured by scanning on the Odyssey® and results shown are mean fluorescence intensities of a duplicate analysis + deviation. Data are from one out of two independent experiments performed with two different batches of NP. Differences in NP-binding and uptake were analyzed applying two-way ANOVA with Bonferroni posttests, * = $P < 0.05$ or *** = $P < 0.0001$.

The *in vivo* uptake was examined by injecting mice s.c. in the flank with NP-CD40 or NP-Iso and the draining inguinal lymph node (LN) excised 48 hr later. Higher amounts of NP-CD40 were taken up by CD11c⁺CD11b⁺F4/80⁻ DC than NP-Iso (Figure 7.2A). In addition, the LN contained significantly higher numbers of NP⁺ DC when NP-CD40 were injected (Figure 7.2B). CD19⁺B220⁺ B cells also internalized NP-CD40 although to a lesser extent than DC (Figure 7.2C and 7.2D). Control injections of NP-Iso mixed with same amount of soluble anti-CD40 showed the necessity of coating the αCD40-mAb to the NP surface. In summary, CD40-targeting of NP improves binding and uptake and facilitates efficient *in vivo* delivery of NP to DC.

Enhanced maturation of DC via CD40-targeted delivery of TLR2 and TLR3 ligands encapsulated in PLGA-NP

The potency of various NP formulations (Table 7.1) to activate DC was studied *in vitro* by analyzing the cell-surface expression of the T cell co-stimulatory molecules CD86 and

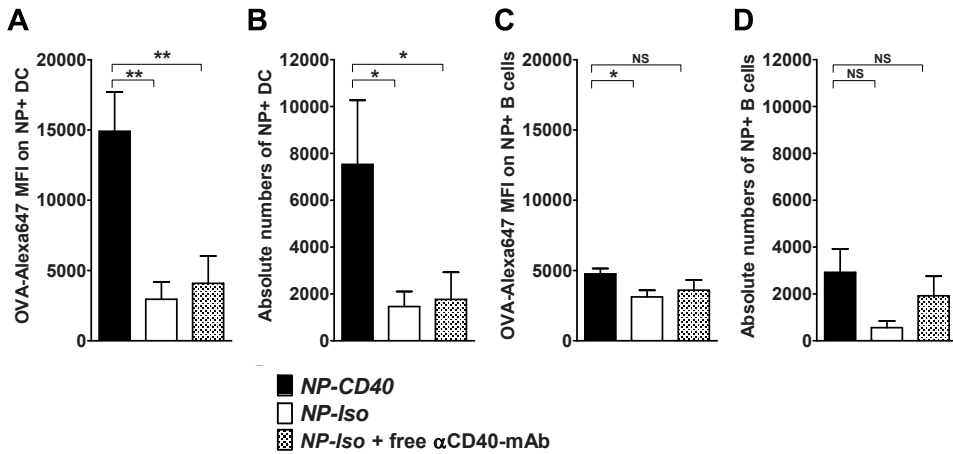


Figure 7.2 NP-CD40 are better targeted *in vivo* to and internalized by DC upon s.c. injection.

WT mice were injected s.c. in the right flank with *NP-CD40* or *NP-Iso* encapsulating 10 μ g OVA-Alexa647 or *NP-Iso* mixed with soluble α CD40. After 48 hr mice were sacrificed and single-cell suspensions prepared from the inguinal LN and stained with fluorescent DC-specific mAb. The different immune cell populations positive for Alexa-647 fluorescence were distinguished by flow cytometry. The absolute numbers of NP⁺ CD11c⁺CD11b⁺F4/80⁺ DC were calculated and the results shown are averages \pm SEM of two independent experiments using 3–5 mice per group (A). Relative amount of particles internalized per cell was based on the Alexa-647 MFI on the NP⁺ DC and values depicted as mean \pm SEM (B). NP⁺ CD19⁺B220⁺ B cells (C) and MFI on the NP⁺ B cells (D) were quantified. The Mann Whitney or the unpaired student's test was used to compare the absolute numbers of NP⁺ cells after vaccinations with *NP-CD40* and *NP-Iso* and the resulting MFI on NP⁺ cells, * = $P < 0.05$ & ** = $P < 0.01$.

CD40 on DC and the capacity of these cells to produce IL-12. The strongest DC maturation resulted from incubation with *NP-CD40* as reflected by the highest production of IL-12, (Figure 7.3A), but also by IL-6 and IL-2 production (data not shown) and the enhanced surface expression of CD86 and CD40 (Figure 7.3B & C). At the concentrations tested, single formulations of (PLGA-Ag/TLRL)-mAb NP containing either Pam3Csk4, Poly(I:C) or FGK45 showed poor (FGK45 & TLR2L), or low (Poly(I:C)) capacity to activate DC compared to NP formulations co-encapsulating Pam3Csk4 and Poly(I:C) (Supporting Information Figure S7.2). Coupling of the α CD40-mAb to NP encapsulating TLRL appeared to be essential to achieve the synergistic activation of DC as *NP-Iso* mixed with soluble (free) α CD40-mAb showed lower potency compared to *NP-CD40* (Figure 7.3D). Furthermore, DC incubated

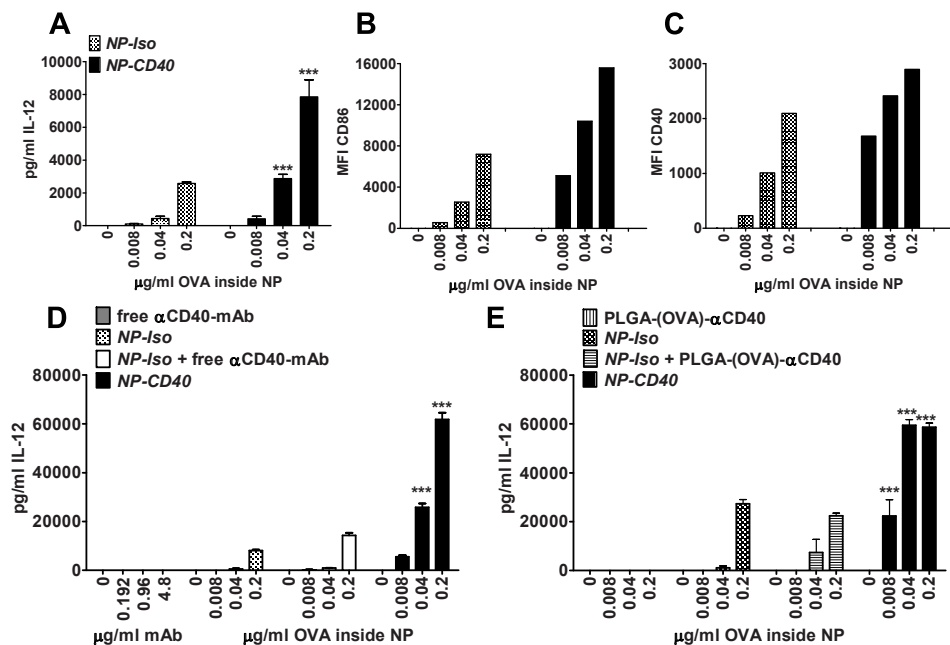


Figure 7.3 CD40-targeted PLGA-(Ag/TLR2+3L) NP show superior capacity to mature DC compared to non-targeted NP.

WT BMDC (100,000 cells/well) were incubated with titrated amounts of *NP-CD40* or *NP-Iso* for 24 hr at 37°C. Culture supernatants were harvested and the amount of IL-12 determined by ELISA (A). Post-incubation, DC were stained with fluorescent antibodies against CD86 (B) and CD40 (C) followed by Flow Cytometry analysis. IL-12 was determined in culture supernatants after 24 hr incubation of DC with *NP-CD40*, *NP-Iso* and control formulations of *NP-Iso* mixed with soluble αCD40 mAb (D) or PLGA-(OVA)-αCD40 NP (E). Differences in cytokine production were analyzed applying two way ANOVA with Bonferroni posttests, *** = $P < 0.001$.

with mixtures of *NP-Iso* with PLGA-(Ag)-αCD40 NP (lacking both TLR ligands) did not induce DC maturation to a similar extent as *NP-CD40* (Figure 7.3E). No DC maturation was induced by NP formulations encapsulating just OVA, independent of CD40-targeting (data not shown). We tested up to 25-fold higher amounts of soluble OVA compared to the amount encapsulated in NP, either alone or in combination with TLR and αCD40-mAb but observed no additive stimulatory effect on DC maturation (data not shown). In summary, we show that CD40-targeted delivery of NP, co-encapsulating Poly(I:C) and Pam3Csk4, synergistically enhances DC maturation in contrast to non-targeted NP containing the same Ag/TLRL cargo.

Improved CD4⁺ T cell proliferation and IFN- γ production by NP-CD40

We studied if DC loaded with NP-CD40 resulted in efficient MHC class II Ag processing and activation of naïve CD4⁺ T cells *in vitro*. In line with the previous results, OVA-specific CD4⁺ T cells proliferated better but especially produced significantly higher amounts of IFN- γ when primed by DC loaded with NP-CD40 compared to stimulation by NP-Iso loaded DC (Figure 7.4). In conclusion, CD40-targeted delivery to DC of Pam3Csk4 and Poly(I:C) co-encapsulated with protein Ag in NP, also facilitates MHC class II presentation and enhances effector CD4⁺ T cell functionality. DC loaded with NP-CD40 and NP-Iso both had potent APC capacity resulting in similar proliferation and IFN- γ production by naïve CD8⁺ T cells *in vitro* (data not shown).

Vaccination with NP-CD40 improves CD8⁺ T cell responses

The quantity and quality of TAA-specific CD8⁺ T cells are important determinants for a robust anti-tumor immune response. Enhancing CD8⁺ T cell responses in the presence

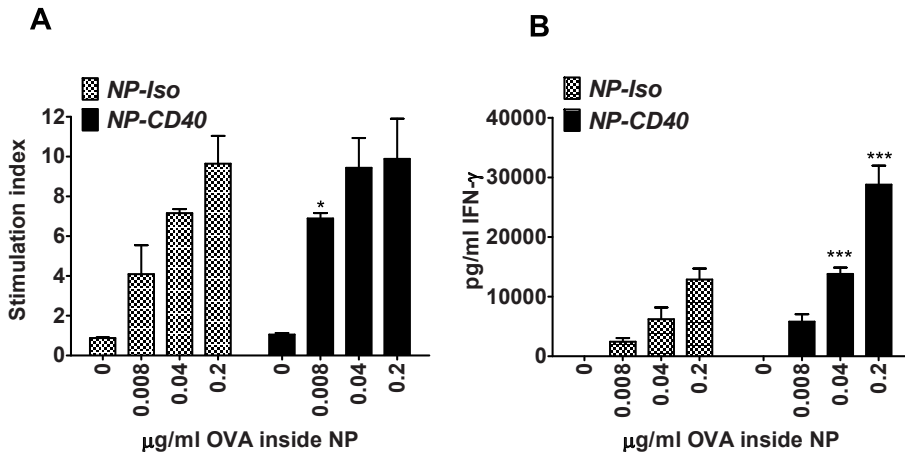


Figure 7.4 DC loaded with NP-CD40 have improved APC-capacity to stimulate CD4⁺ T cell proliferation and IFN- γ production.

BMDC from C57BL/6 were incubated with titrated amounts of NP-CD40 or NP-Iso for 5 hr at 37°C. After incubation with Ag, 75% of the culture medium was removed and splenocytes from OT-II mice added (200000 splenocytes/200 μ l/well). OVA-specific CD4⁺ T cell proliferation was analyzed 72 hr later by analysis of [³H]-thymidine incorporation which was added in the final 16 hours of culture (A). Samples were taken after 48 hr of co-culture between Ag-loaded DC and OT-II splenocytes and analyzed for IFN- γ levels (B). Differences in CD4⁺ T cell proliferation and cytokine production were analyzed using the two way ANOVA with Bonferroni posttests, * = P < 0.5 and *** = P < 0.0001.

of a tumor is a crucial merit of therapeutic vaccines. Therefore, to study how *NP-CD40* modulate an ongoing anti-tumor CD8⁺ T cell response we collected blood samples of tumor-bearing animals 7 days after vaccination. *NP-CD40* significantly boosted the %

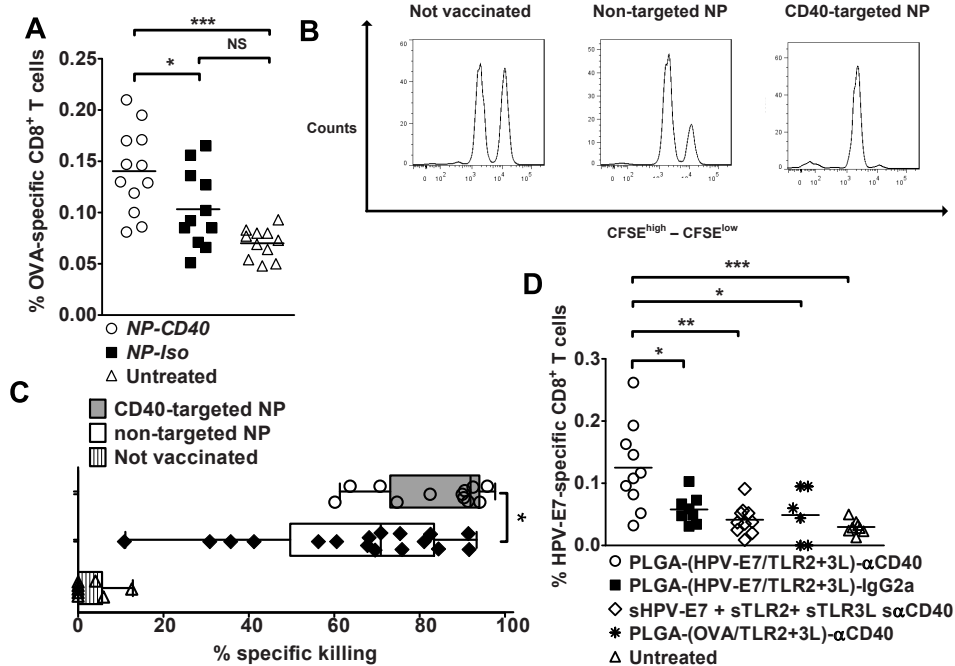


Figure 7.5 Vaccinations with *NP-CD40* prime CD8⁺ T cells with improved cytotoxic capacity compared to *NP-Iso*.

Tail vein blood samples were taken on day 14 post-tumor inoculation from tumor bearing mice which received vaccinations with either *NP-CD40* or *NP-Iso*. Blood samples were prepared as stated in M&M and stained with SIINFEKL-Tetramers to determine OVA-specific CD8⁺ T cells by FACS (**A**) WT mice were vaccinated s.c. with 10 μg OVA encapsulated in CD40-targeted PLGA-(Ag/TLR2+3L) NP or non-targeted PLGA-(Ag/TLR2+3L) control NP in the right flank. On day 7 day post vaccination, SIINFEKL-loaded CFSE^{high} OVA-specific target cells and ASNENMETM-loaded CFSE^{low} INFLUENZA-specific target cells (negative controls) were injected i.v. in a 1:1 ratio and mice sacrificed 18 hr later to determine the degree of OVA-specific lysis of the target cells (**B**). The average % OVA-specific target cell killing, of 3 independent experiments, was quantified as described in M&M (**C**). TC-1 tumor-bearing mice were vaccinated on day 7 with NP-formulations encapsulating 15 μg HPV-E7 protein and TLR or soluble protein/TLR mixture. On day 15, tail vein blood samples were collected and the % of RAHYNIVTF/H2-D^b specific CD8⁺ T cells determined (**D**). Differences in % of Ag specific CD8⁺ T cells and *in vivo* killing or target cells were analyzed applying the Mann Whitney tests, * = P < 0.05.

of TAA-specific CD8⁺ T cells compared to *NP-Iso* vaccinated and untreated mice (Figure 7.5A). Ag-specific CD8⁺ T cells after vaccination of naïve animals with *NP-CD40* showed strong *in vivo* cytotoxic capacity (Figure 7.5B), which resulted in efficient killing of target cells (Figure 7.5C). Similarly, CD40-targeted NP encapsulating HPV-E7 protein significantly enhanced RAHYNIVTF-specific CD8⁺ T cells in blood after a single vaccination compared to non-targeted NP formulations or a mixture of soluble HPV-E7-protein and adjuvants. Encapsulation of specific Ag in CD40-targeted NP was required for the observed T cell priming as TLRL and an irrelevant protein targeted to CD40 failed to boost HPV-E7 specific responses (Figure 7.5D). NP formulations with no or only one TLRL were inferior vaccines as compared to *NP-CD40* (Supporting Information Figure S7.3). These observations show significant improvement of CD8⁺ T cell quantity and functional quality via CD40-targeted NP-vaccines.

CD40-targeting of NP improves anti-tumor vaccine potency

The prophylactic vaccine potency of NP-vaccines was studied in a murine melanoma-OVA model. Mice were vaccinated or left un-treated and 7 days later challenged with B16-OVA tumors. But both NP-vaccines inhibited tumor growth (Figure 7.6A) and exhibited similar efficacy ($P < 0.001$) in prolonging animal survival compared to un-treated mice (Figure 7.6B). Single TLRL NP-vaccines also induced partial protection against tumor challenge, however; *NP-CD40* inhibited tumor out growth in 50% of tumor bearing animals resulting in the longest median survival time compared to animals vaccinated with the other NP-vaccines (Supporting Information Figure S7.4).

The therapeutic vaccine potency of *NP-CD40* and *NP-Iso* was assessed by vaccinating tumor-bearing mice on day 7 and 17 post tumor inoculation. Comparison based on average tumor size per group could be determined until day 22; hereafter the first animals were sacrificed because of tumor burden. *NP-CD40* vaccinated animals displayed statistically smaller tumors compared to non-treated ($P < 0.01$) and *NP-Iso* treated animals ($P < 0.05$) (Figure 7.6D). Furthermore, *NP-CD40* vaccinated animals displayed a better prolonged survival compared to the control groups ($P < 0.02$) (Figure 7.6D). Collectively, the results indicate that CD40-targeting of PLGA-(Ag/TLR2+3L)-NP potentiates vaccine efficacy and induces (or boosts) anti-tumor responses inhibiting tumor growth and prolonging survival of animals.

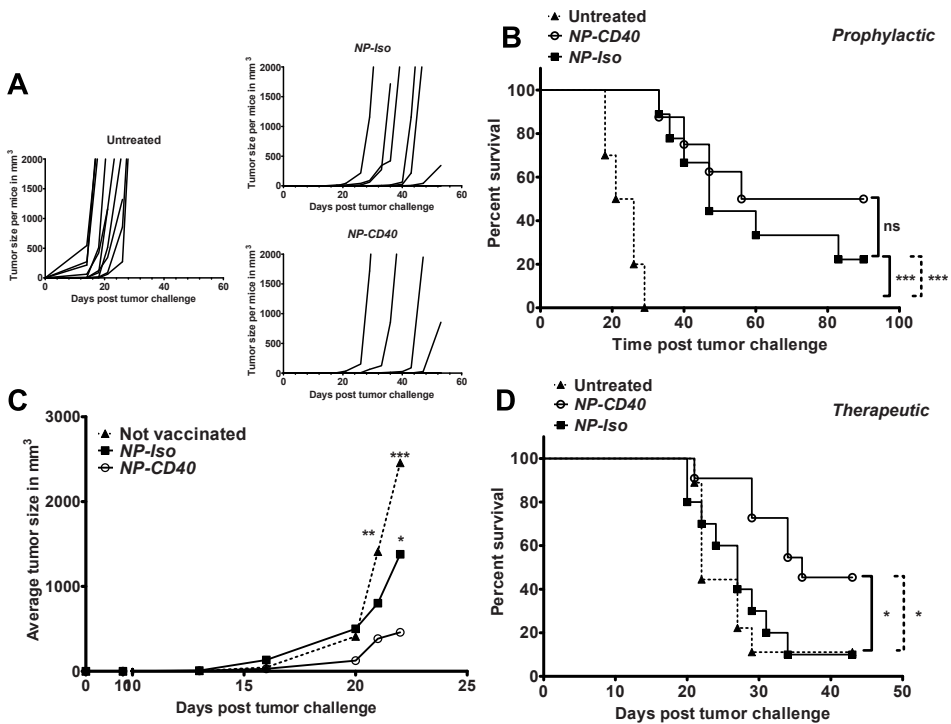


Figure 7.6 Vaccinations with PLGA-(Ag/TLR2+3L)-αCD40 NP induce potent anti-tumor responses.

WT mice were vaccinated in the right flank with 10 μg OVA encapsulated in *NP-CD40* and *NP-Iso* on day 0 or left untreated. On day 7 post-vaccination 2×10^5 B16-OVA tumor cells were inoculated s.c. on the opposite flank. Tumor growth (**A**) and animal survival (**B**) were monitored. Untreated animals were all required to be sacrificed because of tumor burden by day 29. 2×10^5 B16-OVA tumor cells were inoculated s.c. in the left flank of WT mice and these rested for 1 week followed by vaccinations on day 7 and 17 with 10 μg OVA encapsulated in NP. Average tumor size per group was followed in time until day 22, the final time point when all animals were still alive (**C**), and survival monitored (**D**). Differences in tumor sizes per group were determined by regular two-way ANOVA with Bonferroni posttests to calculate the difference in mean values at each time point. Animal survival per group was assessed using Log-rank (Mantel-Cox) test, *** = $P < 0.001$, ** = $P < 0.01$ and * = $P < 0.05$.

Discussion

In this study we formulated a PLGA-NP based multi-compound particulate vaccine which target DC and deliver protein Ag and adjuvants via the cell-surface molecule CD40 with

the aim to activate efficient cytotoxic CD8⁺ T cell responses. The effects of CD40-targeting on vaccine potency were evaluated using a murine melanoma tumor model.

The results described here indicate that the selective and efficient *in vivo* delivery of particulate NP-vaccines to DC via CD40 is feasible and results in efficacious T cell responses. Combined CD40-targeting with TLR2- and TLR3-triggering synergistically enhanced IL-12 production by DC and IFN- γ production by CD4⁺ T cells *in vitro*, suggesting that NP-CD40 facilitates a TH1-mediated pro-inflammatory immune response. TH1 immune polarization by vaccines is essential to sustain robust anti-tumor CD8⁺ T cell responses *in vivo*²⁴. In line with this direct vaccinations with NP-CD40 improved the induction of Ag-specific cytotoxic CD8⁺ T cells and tumor-control.

The covalent coupling of the α CD40-mAb to the NP (NP-CD40) greatly enhanced the maturation effect of the NP-vaccine on DC (Figure 7.3). The better capacity of NP-CD40 to mature DC is possibly a consequence of triggering distinct adapter proteins involved in signaling pathways upstream of NF- κ B transcription regulation of DC maturation; TRAF (CD40)²⁵, MyD88 (TLR2) and TRIF (TLR3)²⁶. Another possibility is that receptor-mediated internalization via CD40 leads to higher quantities of Poly(I:C) and Pam3Csk4 inside intracellular compartments of DC compared to non-targeted NP¹³ inducing stronger TLR-stimulation. Additional experiments are ongoing to elucidate the mechanisms responsible for the enhanced DC maturation by NP-CD40.

Enhanced vaccine-delivery to DC can also be achieved via passive targeting by modifying the size of the vaccine which influences lymph node drainage of the vaccine²⁷. Alternatively, active vaccine-targeting strategies via CD40, as shown in this study, or through C-type lectins such as DEC-205, DC-SIGN and Glec9a greatly improves Ag delivery, processing and T cell priming by DC over non-targeted controls^{14,16,23,28,29}.

It is clear that DC express many cell-surface molecules which can function as potential targets for vaccine-delivery resulting in improved binding and internalization of the vaccine. The cell-surface molecule chosen is based on the DC-subtype possessing the optimal APC-properties for the desired type of immune response³⁰ one aims to activate. Figdor and colleagues have recently questioned the necessity to target vaccines to specific DC-subsets³¹, even though some DC-subtypes can possess a specialized role in peripheral tolerance^{32,33} or in the activation of CD8⁺ T cell mediated immune responses³⁴. However, owing to the plasticity in function of several DC-subtypes^{35,36} and on the results described here and published previously by our group³⁷ we hypothesize that the success

of therapeutic vaccinations is not critically dependent on the DC-subtype targeted but rather on the efficient delivery of the vaccine and importantly the adjuvants in sufficient amounts to activate CD11c⁺ DC instead of non-professional APC.

We recently performed a study using PLGA-(Ag/TLR3+7L)-NP and compared the delivery to DC via the targeting of CD40, CD11c or DEC-205. Our results indicate that the binding and internalization of the NP via these molecules similarly facilitate DC maturation *in vitro* but that CD40-targeting leads to slightly better CD8⁺ T cell responses *in vivo* (L.Cruz & R.Rosalia et al., manuscript in press 10.1016/j.jconrel.2014.07.040).

The surface expression of most targeting molecules is promiscuous on several immune cells. CD40 expression is not restricted to DC. For example, B cells also express CD40 and therefore might contribute to the anti-tumor responses observed after vaccinations with NP-CD40. A small percentage of B cells bind NP *in vivo*, however due to their inferior endocytic capacity³⁸ and T cell activating capacity³⁹ compared to DC it is likely that T cell stimulation by B cells *in vivo* played a minor role in this study.

PLGA-particles were shown to be internalized by M ϕ *in vivo* leading to cross-presentation of particle-encapsulated protein and priming of CD8⁺ T cells⁴⁰. We observed that M ϕ poorly internalized NP-CD40 and NP-Iso compared to DC (data not shown) likely because of the PEG-layer on the NP which blocks non-specific phagocytosis⁴¹. Targeting to CD40 did not lead to better *in vivo* internalization of NP-CD40 by M ϕ and we observed that CD11c⁺CD11b⁺F4/80⁻ DC have higher cell-surface expression of CD40 compared to CD19⁺B220⁺ B cells and CD11c⁺CD11b⁺F4/80⁺ M ϕ (data not shown). The higher CD4-expression on DC may form a mechanistic basis for the improved *in vivo* delivery of NP-CD40 compared to other APC.

Lymphoid organ resident CD8 α ⁺ DC are considered the main Ag cross-presenting and CD8⁺ T cell priming DC in the mouse⁴². We observed a trend that CD8 α ⁺ DC more efficiently internalized NP (Supporting Information Figure S7.1) than CD8 α ⁻ DC. A surprising finding as CD8⁺ and CD8⁻ CD11c⁺ DC were shown to possess similar phagocytic capacity⁴³, but differed in the mechanisms and efficiency of Ag-presentation⁴⁴. Cell-surface expression of CD40 was reported to be higher on CD8 α ⁺ DC in mice⁴⁵ which could explain why more CD8 α ⁺ DC internalize higher numbers of NP-CD40 via receptor mediated endocytosis.

CD40 seems to be a suitable target to deliver other types of particulate vaccines. Similar *ex vivo* and *in vivo* DC-specific delivery of a CD40-targeted adenoviral tumor vaccine was previously reported⁴⁶ inducing stronger anti-tumor responses than the non-targeted

vectors, which supports CD40 on DC to be a suitable target to deliver not only PLGA-NP based vaccines but also other types of particulate vaccines.

DC were poorly matured by (PLGA-Ag)- α CD40 NP or soluble α CD40-mAb in the absence of TLRL. This was surprising as α CD40-mAb bound to polystyrene⁴⁷, poly(γ -glutamic acid)⁴⁸ and porous silicon NP⁴⁹ resulted in DC maturation. FGK45 is a relatively weaker DC activating adjuvant compared to most TLRL⁵⁰ and we hypothesized that coupling of α CD40-mAb to PLGA-NP would improve the cross-linking of CD40 on DC and enhance the stimulatory effect of FGK45. But, our data suggests that the stimulating properties of FGK45 coupled to PLGA-NP at the quantities tested were insufficient to strongly activate DC as a single adjuvant. Higher concentrations of FGK45, than reported in our study, coupled to NP could not be achieved due to already saturating amounts of the mAb coupled to the NP-surface. Of course, increasing the size (Table 7.1) of the NP would allow the coupling of more antibodies, but we opted not to as the amounts of α CD40-mAb coupled to the NP were already sufficient to significantly boost the immune activating properties of TLRL encapsulated in NP. And importantly, higher dosages of systemic α CD40-mAb after injection might lead to liver toxicity as reported recently by Fransen et al.⁵¹. Vaccinations using NP-CD40 resulted in the most efficient T cell responses *in vitro* and *in vivo*. Multi-adjuvant vaccines are known to improve immune responses compared to single adjuvant based vaccines⁵² and Berzofsky et al. recently showed that this effect is related to a qualitative differences of the primed effector T cells⁵³. Our observations support this report as the strongest CD8⁺ T cell cytotoxicity was achieved with vaccines combining TLR2L, TLR3L and α CD40-mAb.

Efficient and potent therapies against infectious diseases and cancer are highly necessary in the clinic. With recent exciting developments in immunotherapy, active vaccinations are close to being implemented as an accepted anti-cancer therapy but also against infectious diseases, for example Influenza⁵⁴. However, fine-tuning is required to achieve maximum vaccine potency via DC-controlled anti-tumor immune responses. We show here that CD40-targeting is an attractive strategy to deliver PLGA-NP-based well-defined vaccines to CD11c⁺ DC resulting in significant tumor control. Using the TC-1 tumor model, we showed in a clinically-relevant Ag model that CD40-targeting enhances HPV-E7 specific CD8⁺ T cell responses (Figure 7.5D) suggesting broad applicability of CD40-targeted NP-vaccines to boost immune responses against other TAA. But possibly also as therapy for other diseases caused by microorganisms with known Ag-specificity, for example the parasite *Plasmodium vivax* which causes malaria.

In conclusion, significant boosting of effector T cells is achieved by improving the delivery of PLGA-(Ag/TLR2+3L) NP to DC via CD40 targeting. DC efficiently internalized the vaccine leading to full blown maturation and efficient priming of CD8⁺ T cells which led to prolonged survival of tumor-bearing animals.

Acknowledgements

Financial support for this study was provided by the clinical pharmacy and toxicology department of the Leiden University Medical Center

References

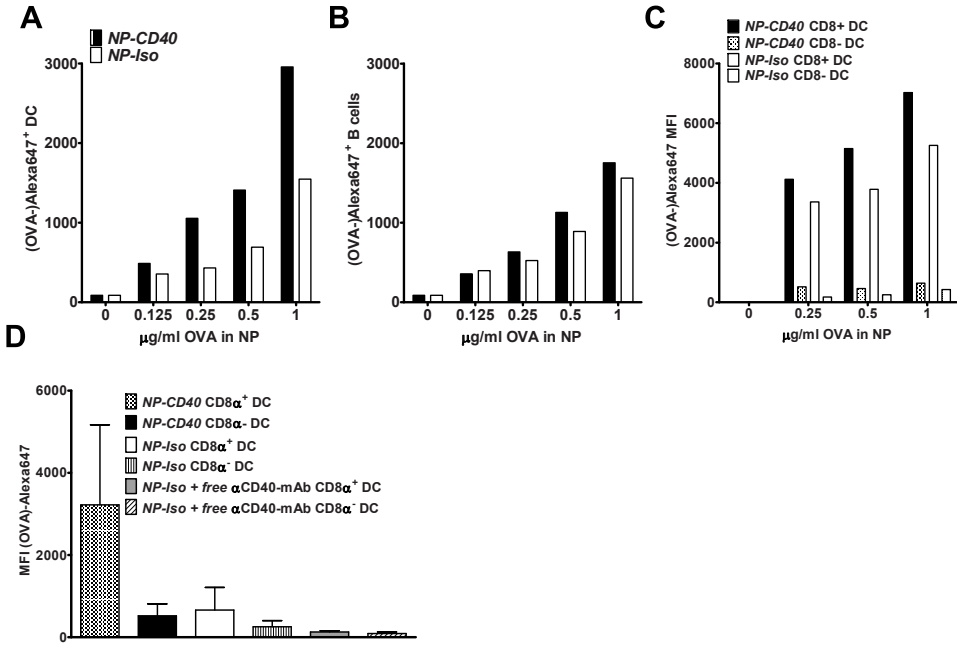
1. Palucka K, Ueno H, Fay J, Banchereau J 2011. Dendritic cells and immunity against cancer. *Journal of Internal Medicine* 269(1):64-73.
2. Banchereau J, Steinman RM 1998. Dendritic cells and the control of immunity. *Nature* 392(6673):245-252.
3. Palucka K, Banchereau J 2012. Cancer immunotherapy via dendritic cells. *Nature Reviews Cancer* 12(4):265-277.
4. Pasare C, Medzhitov R 2005. Toll-like receptors: linking innate and adaptive immunity. *Adv Exp Med Biol* 560:11-18.
5. Tacken PJ, de Vries IJ, Torensma R, Figdor CG 2007. Dendritic-cell immunotherapy: from ex vivo loading to in vivo targeting. *Nature Reviews Immunology* 7(10):790-802.
6. Melief CJ 2008. Cancer immunotherapy by dendritic cells. *Immunity* 29(3):372-383.
7. Shen H, Ackerman AL, Cody V, Giodini A, Hinson ER, Cresswell P, Edelson RL, Saltzman WM, Hanlon DJ 2006. Enhanced and prolonged cross-presentation following endosomal escape of exogenous antigens encapsulated in biodegradable nanoparticles. *Immunology* 117(1):78-88.
8. Fischer S, Schlosser E, Mueller M, Csaba N, Merkle HP, Groettrup M, Gander B 2009. Concomitant delivery of a CTL-restricted peptide antigen and CpG ODN by PLGA microparticles induces cellular immune response. *Journal of Drug Targeting* 17(8):652-661.
9. Silva AL, Rosalia RA, Sazak A, Carstens MG, Ossendorp F, Oostendorp J, Jiskoot W 2013. Optimization of encapsulation of a synthetic long peptide in PLGA nanoparticles: low-burst release is crucial for efficient CD8(+) T cell activation. *European Journal of Pharmaceutics and Biopharmaceutics* 83(3):338-345.
10. Silva JM, Videira M, Gaspar R, Preat V, Florindo HF 2013. Immune system targeting by biodegradable nanoparticles for cancer vaccines. *Journal of Controlled Release* 168(2):179-199.
11. Mueller M, Schlosser E, Gander B, Groettrup M 2011. Tumor eradication by immunotherapy with biodegradable PLGA microspheres--an alternative to incomplete Freund's adjuvant. *Int J Cancer* 129(2):407-416. doi: 410.1002/ijc.25914. Epub 22011 Mar 25928.
12. Bazile D, Prud'homme C, Bassoullet MT, Marlard M, Spenlehauer G, Veillard M 1995. Stealth Me.PEG-PLA nanoparticles avoid uptake by the mononuclear phagocytes system. *Journal of Pharmaceutical Sciences* 84(4):493-498.
13. Tacken PJ, Zeelenberg IS, Cruz LJ, van Hout-Kuijter MA, van de Glind G, Fokkink RG, Lambeck AJ, Figdor CG 2011. Targeted delivery of TLR ligands to human and mouse dendritic cells strongly enhances adjuvanticity. *Blood* 118(26):6836-6844. doi: 6810.1182/blood-2011-6807-367615. Epub 362011 Oct 367613.
14. Macho-Fernandez E, Cruz LJ, Ghinnagow R, Fontaine J, Bialecki E, Frisch B, Trottein F, Faveeuw C 2014. Targeted Delivery of alpha-Galactosylceramide to CD8alpha+ Dendritic Cells Optimizes Type I NKT Cell-Based Antitumor Responses. *Journal of Immunology* 193(2):961-969.

15. Hamdy S, Haddadi A, Shayeganpour A, Samuel J, Lavasanifar A 2011. Activation of antigen-specific T cell-responses by mannan-decorated PLGA nanoparticles. *Pharm Res* 28(9):2288-2301. doi: 2210.1007/s11095-11011-10459-11099. Epub 12011 May 11011.
16. Han R, Zhu J, Yang X, Xu H 2011. Surface modification of poly(D,L-lactic-co-glycolic acid) nanoparticles with protamine enhanced cross-presentation of encapsulated ovalbumin by bone marrow-derived dendritic cells. *Journal of Biomedical Materials Research Part A* 96(1):142-149.
17. Schoenberger SP, Toes RE, van der Voort EI, Offringa R, Melief CJ 1998. T-cell help for cytotoxic T lymphocytes is mediated by CD40-CD40L interactions. *Nature* 393(6684):480-483.
18. Schuurhuis DH, Laban S, Toes RE, Ricciardi-Castagnoli P, Kleijmeer MJ, van der Voort EI, Rea D, Offringa R, Geuze HJ, Melief CJ, Ossendorp F 2000. Immature dendritic cells acquire CD8(+) cytotoxic T lymphocyte priming capacity upon activation by T helper cell-independent or -dependent stimuli. *The Journal of Experimental Medicine* 192(1):145-150.
19. Cohn L, Chatterjee B, Esselborn F, Smed-Sorensen A, Nakamura N, Chalouni C, Lee BC, Vandlen R, Keler T, Lauer P, Brockstedt D, Mellman I, Delamarre L 2013. Antigen delivery to early endosomes eliminates the superiority of human blood BDCA3+ dendritic cells at cross presentation. *The Journal of Experimental Medicine* 210(5):1049-1063.
20. Schjetne KW, Fredriksen AB, Bogen B 2007. Delivery of antigen to CD40 induces protective immune responses against tumors. *Journal of Immunology* 178(7):4169-4176.
21. Schuurhuis DH, van Montfoort N, Ioan-Facsinay A, Jiawan R, Camps M, Nouta J, Melief CJ, Verbeek JS, Ossendorp F 2006. Immune complex-loaded dendritic cells are superior to soluble immune complexes as antitumor vaccine. *Journal of Immunology* 176(8):4573-4580.
22. Moore MW, Carbone FR, Bevan MJ 1988. Introduction of soluble protein into the class I pathway of antigen processing and presentation. *Cell* 54(6):777-785.
23. Cruz LJ, Tacke PJ, Fokkink R, Joosten B, Stuart MC, Albericio F, Torensma R, Figdor CG 2010. Targeted PLGA nano- but not microparticles specifically deliver antigen to human dendritic cells via DC-SIGN in vitro. *J Control Release* 144(2):118-126. doi: 110.1016/j.jconrel.2010.1002.1013. Epub 2010 Feb 1013.
24. Ossendorp F, Mengede E, Camps M, Filius R, Melief CJ 1998. Specific T helper cell requirement for optimal induction of cytotoxic T lymphocytes against major histocompatibility complex class II negative tumors. *The Journal of Experimental Medicine* 187(5):693-702.
25. Mackey MF, Wang Z, Eichelberg K, Germain RN 2003. Distinct contributions of different CD40 TRAF binding sites to CD154-induced dendritic cell maturation and IL-12 secretion. *European Journal of Immunology* 33(3):779-789.
26. Brown J, Wang H, Hajishengallis GN, Martin M 2011. TLR-signaling networks: an integration of adaptor molecules, kinases, and cross-talk. *Journal of Dental Research* 90(4):417-427.
27. Manolova V, Flace A, Bauer M, Schwarz K, Saudan P, Bachmann MF 2008. Nanoparticles target distinct dendritic cell populations according to their size. *Eur J Immunol* 38(5):1404-1413. doi: 1410.1002/eji.200737984.

28. Raghuwanshi D, Mishra V, Suresh MR, Kaur K 2012. A simple approach for enhanced immune response using engineered dendritic cell targeted nanoparticles. *Vaccine* 30(50):7292-7299.
29. Schreibelt G, Klinkenberg LJ, Cruz LJ, Tacken PJ, Tel J, Kreutz M, Adema GJ, Brown GD, Figdor CG, de Vries IJ 2012. The C-type lectin receptor CLEC9A mediates antigen uptake and (cross-) presentation by human blood BDCA3+ myeloid dendritic cells. *Blood* 119(10):2284-2292.
30. Merad M, Sathe P, Helft J, Miller J, Mortha A 2013. The dendritic cell lineage: ontogeny and function of dendritic cells and their subsets in the steady state and the inflamed setting. *Annu Rev Immunol* 31:563-604.
31. Kreutz M, Tacken PJ, Figdor CG 2013. Targeting dendritic cells--why bother? *Blood* 121(15):2836-2844. doi: 2810.1182/blood-2012-2809-452078. Epub 452013 Feb 452076.
32. Idoyaga J, Fiorese C, Zbytnuik L, Lubkin A, Miller J, Malissen B, Mucida D, Merad M, Steinman RM 2013. Specialized role of migratory dendritic cells in peripheral tolerance induction. *J Clin Invest* 123(2):844-854. doi: 810.1172/JCI65260. Epub 62013 Jan 65269.
33. Gottschalk C, Damuzzo V, Gotot J, Kroczek RA, Yagita H, Murphy KM, Knolle PA, Ludwig-Portugall I, Kurts C 2013. Batf3-dependent dendritic cells in the renal lymph node induce tolerance against circulating antigens. *Journal of the American Society of Nephrology* 24(4):543-549.
34. Kroczek RA, Henn V 2012. The Role of XCR1 and its Ligand XCL1 in Antigen Cross-Presentation by Murine and Human Dendritic Cells. *Frontiers in Immunology* 3:14.
35. Dresch C, Leverrier Y, Marvel J, Shortman K 2012. Development of antigen cross-presentation capacity in dendritic cells. *Trends in Immunology* 33(8):381-388.
36. Shortman K, Liu YJ 2002. Mouse and human dendritic cell subtypes. *Nature Reviews Immunology* 2(3):151-161.
37. van Montfoort N, Mangsbo SM, Camps MG, van Maren WW, Verhaart IE, Waisman A, Drijfhout JW, Melief CJ, Verbeek JS, Ossendorp F 2012. Circulating specific antibodies enhance systemic cross-priming by delivery of complexed antigen to dendritic cells in vivo. *European Journal of Immunology* 42(3):598-606.
38. Rabinovitch M 1995. Professional and non-professional phagocytes: an introduction. *Trends in Cell Biology* 5(3):85-87.
39. Lim TS, Goh JK, Mortellaro A, Lim CT, Hammerling GJ, Ricciardi-Castagnoli P 2012. CD80 and CD86 differentially regulate mechanical interactions of T-cells with antigen-presenting dendritic cells and B-cells. *PLoS One* 7(9):e45185.
40. Schliehe C, Redaelli C, Engelhardt S, Fehlings M, Mueller M, van Rooijen N, Thiry M, Hildner K, Weller H, Groettrup M 2011. CD8- dendritic cells and macrophages cross-present poly(D,L-lactate-co-glycolate) acid microsphere-encapsulated antigen in vivo. *Journal of Immunology* 187(5):2112-2121.
41. Gref R, Luck M, Quelled P, Marchand M, Dellacherie E, Harnisch S, Blunk T, Muller RH 2000. 'Stealth' corona-core nanoparticles surface modified by polyethylene glycol (PEG): influences of the corona (PEG chain length and surface density) and of the core composition on phagocytic uptake and plasma protein adsorption. *Colloids and Surfaces B, Biointerfaces* 18(3-4):301-313.

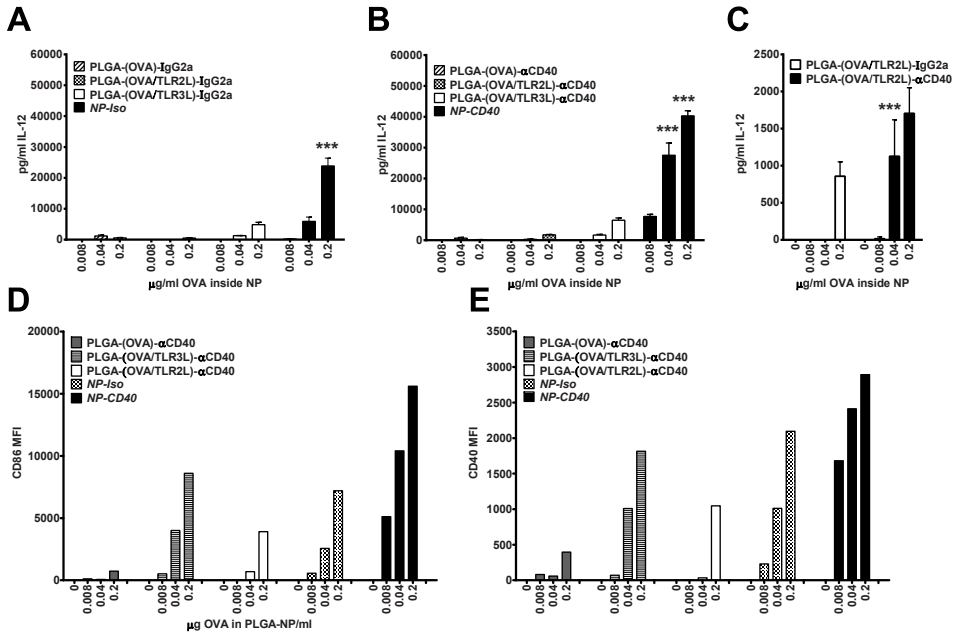
42. Shortman K, Heath WR 2010. The CD8⁺ dendritic cell subset. *Immunological Reviews* 234(1):18-31.
43. Schnorrer P, Behrens GM, Wilson NS, Pooley JL, Smith CM, El-Sukkari D, Davey G, Kupresanin F, Li M, Maraskovsky E, Belz GT, Carbone FR, Shortman K, Heath WR, Villadangos JA 2006. The dominant role of CD8⁺ dendritic cells in cross-presentation is not dictated by antigen capture. *Proceedings of the National Academy of Sciences of the United States of America* 103(28):10729-10734.
44. Kamphorst AO, Guermonprez P, Dudziak D, Nussenzweig MC 2010. Route of antigen uptake differentially impacts presentation by dendritic cells and activated monocytes. *Journal of Immunology* 185(6):3426-3435.
45. Gao X, Wang S, Fan Y, Bai H, Yang J, Yang X 2010. CD8⁺ DC, but Not CD8⁻DC, isolated from BCG-infected mice reduces pathological reactions induced by mycobacterial challenge infection. *PLoS One* 5(2):e9281.
46. Hangalapura BN, Oosterhoff D, de Groot J, Boon L, Tuting T, van den Eertwegh AJ, Gerritsen WR, van Beusechem VW, Pereboev A, Curiel DT, Scheper RJ, de Gruijl TD 2011. Potent antitumor immunity generated by a CD40-targeted adenoviral vaccine. *Cancer Research* 71(17):5827-5837.
47. Kempf M, Mandal B, Jilek S, Thiele L, Voros J, Textor M, Merkle HP, Walter E 2003. Improved stimulation of human dendritic cells by receptor engagement with surface-modified microparticles. *Journal of Drug Targeting* 11(1):11-18.
48. Broos S, Sandin LC, Apel J, Totterman TH, Akagi T, Akashi M, Borrebaeck CA, Ellmark P, Lindstedt M 2012. Synergistic augmentation of CD40-mediated activation of antigen-presenting cells by amphiphilic poly(γ -glutamic acid) nanoparticles. *Biomaterials* 33(26):6230-6239.
49. Gu L, Ruff LE, Qin Z, Corr M, Hedrick SM, Sailor MJ 2012. Multivalent porous silicon nanoparticles enhance the immune activation potency of agonistic CD40 antibody. *Advanced Materials (Deerfield Beach, Fla)* 24(29):3981-3987.
50. Welters MJ, Bijker MS, van den Eeden SJ, Franken KL, Melief CJ, Offringa R, van der Burg SH 2007. Multiple CD4 and CD8 T-cell activation parameters predict vaccine efficacy in vivo mediated by individual DC-activating agonists. *Vaccine* 25(8):1379-1389.
51. Fransen MF, Sluijter M, Morreau H, Arens R, Melief CJ 2011. Local activation of CD8 T cells and systemic tumor eradication without toxicity via slow release and local delivery of agonistic CD40 antibody. *Clinical Cancer Research* 17(8):2270-2280.
52. Kasturi SP, Skountzou I, Albrecht RA, Koutsonanos D, Hua T, Nakaya HI, Ravindran R, Stewart S, Alam M, Kwissa M, Villinger F, Murthy N, Steel J, Jacob J, Hogan RJ, Garcia-Sastre A, Compans R, Pulendran B 2011. Programming the magnitude and persistence of antibody responses with innate immunity. *Nature* 470(7335):543-547.
53. Zhu Q, Egelston C, Gagnon S, Sui Y, Belyakov IM, Klinman DM, Berzofsky JA 2010. Using 3 TLR ligands as a combination adjuvant induces qualitative changes in T cell responses needed for antiviral protection in mice. *The Journal of clinical investigation* 120(2):607-616.
54. Slutter B, Pewe LL, Lauer P, Harty JT 2013. Cutting edge: rapid boosting of cross-reactive memory CD8 T cells broadens the protective capacity of the Flumist vaccine. *Journal of immunology* 190(8):3854-3858.

Supporting Information



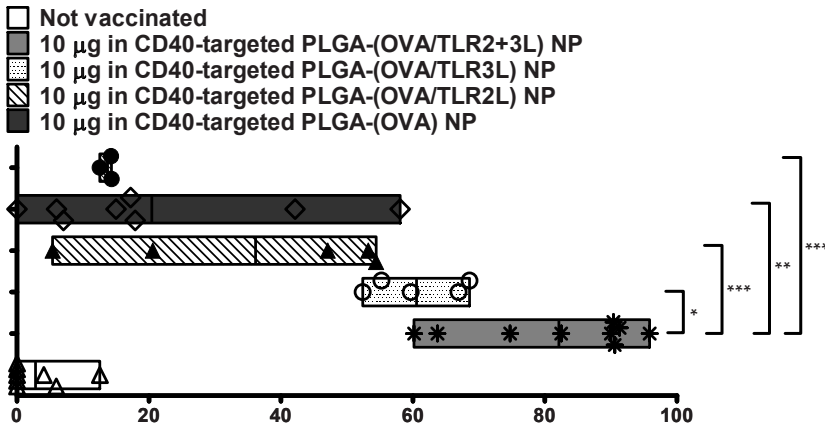
Supporting Information Figure S7.1 DC and B Cells internalize NP-CD40 and NP-Iso in vitro and NP-CD40 are preferentially internalized by CD8⁺CD11⁺ DC.

Splenocytes were for 1 hr with (200,000 cells/well of a 96-wells plate) with titrated (2-step dilutions based on encapsulated OVA-protein in NP) amounts of PLGA-(OVA/TLR2+3L)- α CD40 or PLGA-(OVA/TLR2+3L)-IgG2a NP containing OVA-Alexa647. Cells were kept cold after incubation, washed 3x with PBS to remove unbound NP. Cells were then stained with antibodies against various cell surface molecules and analyzed by flow cytometry DC were designated as CD3⁺F4/80⁻CD11b⁺CD11c⁺ (**A**) or divided into CD8⁺ or CD8⁻ cells (**C**). B cells were gated as CD3⁺CD19⁺B220⁺ cells (**B**). NP encapsulated was determined based on the OVA-Alexa647 fluorescence intensity. C57BL/6 animals were vaccinated s.c. in the right flank with 10 μ g OVA-Alexa647 encapsulated in NP and sacrificed 48 hr post-vaccination and the inguinal LN harvested and single-cell suspensions, stained with various fluorescent antibodies to distinguish the different immune cell populations which are positive for Alexa-647 fluorescence by Flow Cytometry (**D**).



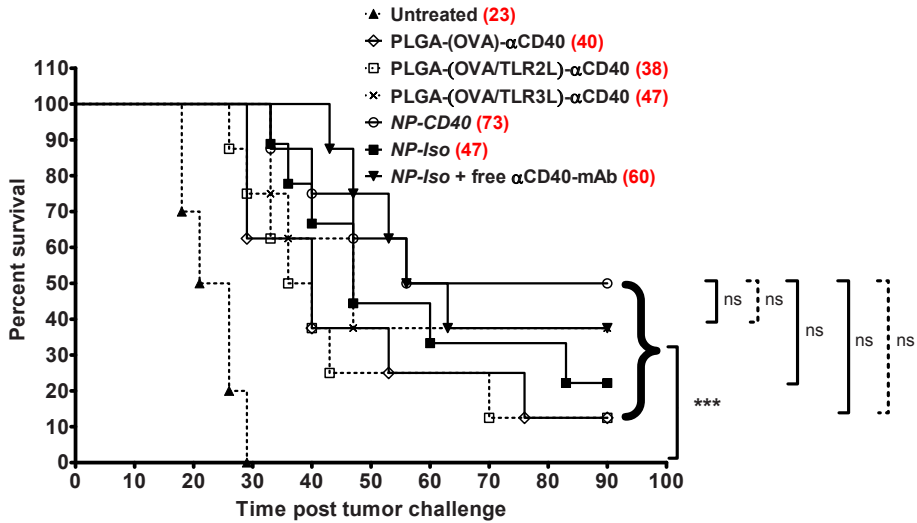
Supporting Information Figure S7.2 Combining triplicate adjuvants (TLR2L, TL3L and $\alpha\text{CD40-mAb}$) leads to strong synergistic activation of DC compared to singlet or doublet adjuvant combinations.

WT BMDC (100,000 cells/well) were incubated with titrated amounts of various PLGA-NP formulations encapsulating TLR2L, TLR3L or $\alpha\text{CD40-mAb}$. Culture supernatants were harvested and the amount of IL-12 determined by ELISA (**A**, **B** and **C**). Post-incubation, DC were stained with fluorescent antibodies against CD86 (**D**) and CD40 (**E**) followed by Flow Cytometry analysis. Differences in cytokine production were analyzed applying two way ANOVA with Bonferroni posttests, *** = $P < 0.001$.



Supporting Information Figure S7.3 CD40-targeted delivery of two TLR co-encapsulated with protein Ag in NP results in superior priming of effector CD8⁺ T cells.

C57BL/6 were vaccinated s.c. in the right flank with 10 µg OVA encapsulated in various CD40-targeted PLGA-(Ag/TLRL) NP formulations. On day 7 day post vaccination, SIINFEKL-loaded CFSE^{high} OVA-specific target cells and ASNENMETM-loaded CFSE^{low} INFLUENZA-specific target cells (negative controls) were injected i.v. in a 1:1 ratio. Mice were sacrificed 18 hr later and the degree of OVA-specific lysis of the target cells determined by FACS and the % killing of OVA-specific target cells quantified as described in M&M. Differences in *in vivo* cytotoxicity of primed CD8⁺ T cells were analyzed applying the Mann Whitney tests, *** = P < 0.001, ** = P < 0.01 & * = P < 0.05.



Supporting Information Figure S7.4 Vaccinations with PLGA-(Ag/TLRL)-mAb NP prolong survival of tumor challenged animals.

C57BL/6 were vaccinated on the right flank with 10 µg OVA encapsulated in different PLGA-(Ag/TLRL)-mAb NP formulations (Table 7.1 manuscript). On day 7 post-vaccination 2×10^5 B16-OVA tumor cells were inoculated s.c. on the opposite flank. Tumor growth was followed and animal survival in the treatment groups were assessed and compared to untreated animals. Untreated animals were all required to be sacrificed because of tumor burden by day 29. Animal survival per group was assessed and differences between the different groups were calculated using Log-rank (Mantel-Cox) test. *** = $P < 0.0001$ for animals treated with the different PLGA-(Ag/TLRL)-mAb NP formulations vs untreated. Numbers in red indicate median survival in days.

